Journal Pre-proof

Size effects of tin oxide quantum dot gas sensors: From partial depletion to volume depletion

Jianqiao Liu, Jiarong Lv, Jingcheng Shi, Liting Wu, Ningning Su, Ce Fu, Qianru Zhang

PII: S2238-7854(20)32073-1

DOI: https://doi.org/10.1016/j.jmrt.2020.11.107

Reference: JMRTEC 2497

To appear in: *Journal of Materials Research and Technology*

Received Date: 3 August 2020

Revised Date: 10 November 2020

Accepted Date: 30 November 2020

Please cite this article as: Liu J, Lv J, Shi J, Wu L, Su N, Fu C, Zhang Q, Size effects of tin oxide quantum dot gas sensors: From partial depletion to volume depletion, *Journal of Materials Research and Technology*, https://doi.org/10.1016/j.jmrt.2020.11.107.

Size effects of tin oxide quantum dot gas sensors: From partial depletion to volume depletion

Jianqiao Liu [1,2,*], Jiarong Lv [2], Jingcheng Shi [2], Liting Wu [2], Ningning Su [2], Ce Fu [2,*], Qianru Zhang [1,*]

1. Institute of Agriculture Resources and Regional Planning, Chinese Academy of Agricultural Sciences, Beijing 100081, China P.R.

2. College of Information Science and Technology, Dalian Maritime University, Dalian 116026, Liaoning, China P.R.

Abstract

The grain size effect is one of the fundamental characteristics of semiconductor gas sensors. However, it has not been fully understood due to the absence of studies on the volume-depleted grains. In this work, the gas-sensitive SnO_2 quantum dots (QDs) from partial depletion to volume depletion are prepared to discuss the size effects. A facile aqueous-based method is used to prepare the size-controllable SnO_2 QDs of 2.0-12.6 nm. The resistance shows a monotonically negative size effect while the response reaches the optimization when the grain radius is comparable to the depletion layer width. It is suggested that the design of highly sensitive gas sensors should consider the equal importance of the control of grain size and depletion layer width. The computational results illustrate size-dependent energy level of donors and number of quasi-free electrons, which are responsible for the negative size effect of resistivity in the volume-depleted SnO_2 crystallites. This work provides a comprehensive understanding of grain size effects from partial depletion to volume depletion in semiconductor gas sensors.

Keywords: size effect; tin oxide quantum dot; gas sensor; volume depletion; receptor function

Corresponding author: Jianqiao Liu, Ce Fu and Qianru Zhang

Email: jqliu@dlmu.edu.cn (J. Liu), fu_ce@dlmu.edu.cn (C. Fu) and zhangqianru@caas.cn (Q. Zhang)

Tel: +86 411 84729934

Fax: +86 411 84729934

Address: College of Information Science and Technology, Dalian Maritime University, Linghai Road 1, Ganjingzi District, Dalian 116026, Liaoning, China P.R.

1. Introduction

Since its first invention in 1962 [1], tin oxide (SnO_2) semiconductor gas sensors have been widely used in many fields, such as the gas leakage alarm in exploration of mine and petroleum [2], environment monitoring [3] and safety control in houses and factories [4]. Along with the minimization of electronic devices during the last decade, the SnO_2 gas sensors experienced the development history from semiconductor bulks [5], thick films [6], thin films [7] to nanostructured devices [8]. Recently, zero-dimensional quantum dots (QDs) also revealed a prospective application in gas-sensing devices [9-12]. The reduced dimensions of electronic elements requested a shrink of semiconductor grains and further investigations demonstrated that the gas-sensing properties were beneficial from such reduction of grain size. Therefore, the grain size effect attracted attentions from the researchers, who were dedicated to the fabrication of high performance gas sensors. These advanced devices were able to operate at room temperature by the chemi-resistive effect taking place on the surface of grains, where the adsorbed oxygen was consumed by the reducing gas molecules or oxidizing gas molecules made competitive adsorption against oxygen adsorbates [13-16].

The grain size effect of SnO_2 gas sensors was first discovered by C. Xu's report in 1991 [17]. It concluded that the gas-sensing properties of resistance and response increased with the reducing grain size. They had a dramatic increase when the grain radius (R_C) was comparable to the depletion layer width (w). A neck-controlled model was therefore proposed to quantitatively describe the size-dependent sensor response. From then on, a series of investigations were completed [18-22]. T. Kida synthesized SnO_2 nanoparticles by seed-mediated growth and studied the properties of gas-sensing films with controlled particle sizes from 7 to 18 nm. The size of

pores among grains was found to be one of the key factors that determined the response of sensors [23]. The size effects of SnO_2 nano-particles were also reported by K. Suematsu, who changed the depletion layer width by controlling the partial pressure of oxygen [24]. These studies illustrated the experimental correlation between grain size and gas-sensing properties of SnO_2 devices, revealing that the resistance and response were of negative dependence on the grain size. Meanwhile, some contributions from the theoretical angle provided further discussions on the knowledge of the grain size effect [25-28]. In the theory of power law of semiconductors, N. Yamazoe provided the size effects of gas-sensing properties to oxygen, reducing gases and oxidizing gases [29]. The theory made a modification on the interpretation of the size effect [30]. In the model of gradient-distributed oxygen vacancies [31,32], the size effects of SnO_2 grains with partial and volume depletion were quantitatively concluded. The model forecasted that the reduced resistance and response were of negative size effects in partial depleted grains while the size effects reversed to be positive in the grains with volume depletion. However, the latter situation was not validated by experimental conclusions.

Indeed, the size effect was ascribed to the proportion of the depletion layer in a semiconductor grain. It was known that the depletion layer formed after the oxygen species adsorbed on the grain surface and seized free electrons from a certain depth. The width of depletion layer was determined by several factors, such as the density of acceptor states on grain surface, the density of ionized donors and the operating temperature. Therefore, it could vary in different circumstances [17] or be controlled by doping techniques [33]. The width of depletion layer for SnO_2 was evaluated to be 3-4.2 nm by C. Xu [17] and J. Liu [33,34] and these values were generally accepted. However, C. Malagu concluded a much greater value of 14.4 nm [35]. Due to

the finite distance that an individual adsorbed oxygen could reach to capture free electrons and the lack of electron supply from the grain bulk [29], the depletion layer width was considered as a constant at specific circumstances. The value of the constant was also used as an essential factor in several theoretical discussions on gas-sensing mechanism of semiconductors, such as the receptor function [36,37], the transducer function [38] and the utility factor [39,40]. The proportion of the depletion layer increased along with the reducing grain radius, illustrating a size effect on sensor resistance and response. In this case ($R_C \geq w$), the grain was partial-depleted. Furthermore, when the grain radius was smaller than the depletion layer width ($R_C < w$), the whole grain reached the status of volume depletion.

The previous studies provided understandings of grain size effect from both experimental and theoretical sides. All of them were succeed in describing the size effect when $R_C \geq w$. However, they failed to make the full image of grain size effect due to the absence of details in the case of volume depletion. The recent development of SnO_2 QD gas sensors, where the grain size was usually smaller than 3 nm, driven the demand of knowledge for the gas-sensing properties of the volume-depleted grains. It is expected to summarize a comprehensive understanding of the grain size effects on semiconductor gas sensors.

In this work, the SnO_2 QDs are prepared in aqueous solution. The hydrothermal treatment is used to control the size of QDs to prepare volume-depleted and partial-depleted grains. Their gas-sensing characteristics are evaluated and correlated with grain size. The first principle calculation based on the density function theory (DFT) is employed to discuss the electron transfer in the computational models. The full image of grain size effect from partial depletion to volume depletion on SnO_2 gas sensors is concluded.

2. Materials and methods

SnO_2 gas-sensing QDs were prepared via a facile bottom-up self-assembly route in aqueous solution [41-43]. Analytical reagents of 2.257 g $SnCl_2 \cdot 2H_2O$ and 0.077 g CH_4N_2S were dissolved into 50 ml deionized water. The solution was stirred in a magnetic stirring apparatus at 25 ^oC for 24 hours and the SnO_2 QDs were obtained after the hydrolysis and oxidation processes. The size of QDs was controlled by the hydrothermal treatment. The QD solution of 10 ml was put into polyphenylene autoclaves, which were heated at 200 ^oC for 0, 4, 8, 12, 16 and 20 hours. The obtained QD powder was washed by deionized water for 3 times and dispersed in deionized water. The Ag interdigital electrodes, as described in Fig. 1(a) [33], were printed on alumina substrates before they were heated at 180 ^oC for 20 min. The QD suspension was spin-coated on the substrates with the spin-coating speed of 1500 rpm. The obtained thin film was dried at 130 ^oC for 10 min. The Ohmic contacts between electrodes and thin films were guaranteed based on the I-V characterization in the previous work [42].

The crystal structures of QD thin films were characterized by X-ray diffraction (XRD) in D/MAX-Ultima (Rigaku, Tokyo, Japan). The high resolution transmission electron microscope (HRTEM, JEM-3200FS, JEOL, Tokyo, Japan) was used to observe the QD morphology. The morphology of the thin film sensor was observed by a scanning electron microscope (SEM, Suppa 55 Sapphire, Carl Zeiss AG, Germany), which involved an energy dispersive spectrometer (EDS) for the element determination. The gas-sensing properties were collected by a computer-controlled characterization system, as shown in Fig. 1(b) [33]. The reducing H_2 gas was used as the target gas, which was injected into the chamber for sensor characterization together with the carrier gas of dry air. During the characterization, the resistance of gas sensor was collected continuously before

and after a series of gas injections. The sensor response (S) was defined as the ratio of the thin film resistance in air (R_a) to the one in the reducing target gas (R_g).

The first principle calculation was carried out to investigate the size effect on the electrical properties of SnO_2 crystallites. The DFT in the Cambridge sequential total energy package (CASTEP) [44] was used. The Perdew-Burke-Ernzerhof (PBE) function was employed to describe the exchange-correlation interaction in the generalized-gradient approximation (GGA). The geometry optimization was conducted to the rutile SnO_2 tetragonal unit cell before it was used to establish structural models. Five super cells were built for SnO_2 crystallites with dimensions of 1×1×2, 2×2×2, 2×2×3, 3×3×3 and 3×3×5. The stoichiometric models were used to evaluate the band structures of SnO_2 super cells, such as the position of conduction band bottom (E_C), valence band top (E_V) as well as the band gap (E_g). It was known that SnO_2 QDs had inherent oxygen vacancies [45] so that 25% of oxygen atoms were removed to create oxygen vacancies inside and on the surface of crystallites. The crystal plane of (110) was then cleaved because it was the least active surface to interact with adsorbed oxygen [46-48]. The oxygen species of O^- [49] was vertically adsorbed on the surface of super cell. These defective models allowed the evaluation of the energy levels provided by the oxygen vacancies and adsorbates after comparing with the stoichiometric models. A vacuum region of 15 Å was used to prevent the interaction between adjacent layers. A 2×2×1 k-point Monkhorst-Pack mesh and an energy cut-off of 340 eV were used. The convergence energy threshold for self-consistent iteration was set to be 10^{-6} eV and the internal stress was less than 0.1 GPa. The density of states (DOS) and Mulliken population distribution were extracted to discuss the electron transfer between Sn and O atoms as well as the electrical properties. The adsorption energy of oxygen species (E_{ads}) was calculated by

$E_{ads}=E_{substrate}+E_{adsorbate}-E_{substrate\text{-}adsorbate}$, where $E_{substrate}$, $E_{adsorbate}$ and $E_{substrate\text{-}adsorbate}$ were the total energy of the super cell, the oxygen adsorbate and the super cell with adsorbed oxygen, respectively [50].

3. Results and discussion

3.1. Structure and morphology

Fig. 2(a) shows the XRD patterns of SnO_2 thin films prepared by QDs with various hydrothermal treatment times. The peaks of (110), (101) and (211) at 26.6°, 33.9° and 51.8° are observed and they are in agreement with the standard pattern of the rutile SnO_2 crystal [51]. The crystallite size of each sample is evaluated by the Scherrer's formula. The ultra-small crystallites grow up during the bottom-up self-assembly process in the hydrothermal treatment. The crystallite size increases from 2 to 8 nm with hydrothermal treatment time but its growth speed slows down after 12 hours, as shown in Fig. 2(b). On the contrary, the HRTEM observations from Fig. 2(d) illustrate a linear relationship between hydrothermal treatment time and grain size of 2.0-12.6 nm. The growth speed is calculated to be 0.5185 nm/h. The different growth correlation between grain size and crystallite size infers that secondary grain boundaries start to appear after hydrothermal treatment of 12 hours. These conclusions have been stated in our previous work [43]. Considering a SnO_2 gas sensor is an assembly of semiconductor grains, the grain size from HRTEM observation is used in the further discussion of size effect. The measurement of grain size from HRTEM is verified by the dynamic light scattering technique in the previous work [41]. Fig. 2(e) shows the SEM observation of the gas sensors, which involves polycrystalline thin films assembled by a great number of SnO_2 QDs. However, the crystallites and the pores among them are too small to be distinguished by the SEM technique. The cross section observation

demonstrates a thickness of 102 nm for the spin-coated SnO_2 QD thin film, as shown in Fig. 2(f). EDS analysis is carried out to determine the elements in the thin film sensors. As shown in Fig. 2(c), only the elements of Sn, O, C and S are detected. It is inferred that C and S are from the remaining source material of CH_4N_2S. The EDS spectrum also makes confirmation that the present SnO_2 thin films are free of Ag incorporation. Therefore, the effect of Ag doping on sensor response [52] is not considered in the discussion of size effect.

3.2. Gas-sensing characteristics

The electrical and gas-sensing properties of SnO_2 QD thin films are tested at the circumstance of room temperature. With the prolongation of hydrothermal treatment time, both of R_a and R_g decrease. Nevertheless, the response to H_2 gas shows a different correlation. It first increases with hydrothermal treatment time, reaching the peak at 12 hours and then turns to descend, as shown in Fig. 3(a), where the H_2 gas concentration is 2740 ppm. The response of SnO_2 QD gas sensor with grain size of 2 nm is 12.6, which is different from the previous work [42] because of the changes in the sensor fabrication process. Fig. 3(b) shows the transient response of the SnO_2 QD thin film with grain size of 2 nm, which is exposed to continuous and repeated injections of 2740 ppm H_2. The thin film sensor shows the good performances of response and repeatability to H_2 gas. The response time (defined as the time that the response rises from 10% to 90% amplitude) is 1066 s and the recovery time (defined as the time that the response descends from 90% to 10% amplitude) is 42 s. The correlation of response against gas concentration is plotted in both linear and logarithmic coordinates. The slope of linear fitting in the logarithmic coordinates is evaluated to be 1.45, which indicates the sensitivity of the SnO_2 QD gas sensor. The value of sensitivity over 1 is much higher than previous gas sensors [8,53-55].

3.3. First principle calculation

To understand the size effect on the electrical properties of SnO_2 gas-sensitive crystallites, the structural models for first principle calculation with various dimensions are established, as shown in Fig. 4, which shows two of them as illustrations. The oxygen species are of stable adsorption on the crystallites because of their positive adsorption energy, as shown in Fig. 5(b). The computational models of stoichiometric super cells are used to evaluate the band structures of the SnO_2 QDs. As shown in the DOS plots in Fig. 5(a), for the stoichiometric super cells, the obvious band gaps are observed between the valence band and the conduction band. The defective models of SnO_2 super cells with adsorbed oxygen are used to simulate actual gas-sensitive crystallites. The DOS plots have significant changes after the introduction of oxygen vacancies and adsorbed oxygen, which bring additional energy levels in the band gap.

The Mulliken population distributions of O and Sn atoms are extracted, as shown in Table 1. In the SnO_2 system, the electron transfer takes place by the donation of Sn atoms and acceptance of O atoms. Taking the model of 1×1×2 super cell as an example, each Sn atom donates 1.65 electrons while each O atom accepts 0.71 electrons. Considering the atom ratio of Sn:O=1:1.5 in the oxygen deficient super cell, there are 0.585 electrons donated by each Sn atom but not accepted by the O atoms. It infers that these 0.585 electrons are quasi-free in the lattice, locating on the energy levels of donors and possibly contributing to the conduction. The number of quasi-free electrons provided by an individual Sn atom decreases with the incremental crystallite size, showing a negative size effect.

3.4. Size effect of grains with partial and volume depletion

The grain size effects on the electrical and gas-sensing properties of SnO_2 QDs are discussed

in both experimental and computational aspects. Therefore, it is possible to make a full image of the size effect for the SnO_2 gas-sensitive nanomaterial, from partial depletion to volume depletion. Fig. 6(a) illustrates the size effect of experimental resistance and response to 2740 ppm H_2 gas when the grain size is within 2-12 nm. As expected, the resistance monotonically increases with the reducing grain size. However, the sensor response to reducing gas is fitted by a volcano-shape curve. This conclusion coincides with the previous result, which is simulated by the model of gradient-distributed oxygen vacancies [56]. If the depletion layer width is 4-4.2 nm [33,34], the response peak locates in region of double depletion layer width. It infers that the response reaches the optimization when R_C=w. Therefore, the control of grain size and depletion layer width are of equal importance for the design of highly sensitive gas sensors. The degradation of sensor performance is observed in the volume-depleted grains. The depletion layer width is recommended to be reduced if ultra-small QDs are used to fabricate gas sensors. The incorporations of pentavalent elements and oxygen vacancies are effective routes to reduce the depletion layer width [17,33].

The computational results are employed to interpret the size effect of electrical properties in volume-depleted grains. It is concluded that quasi-free electrons are provided by Sn atoms. Taking the atom number and cell volume into consideration, the concentration of quasi-free electrons (n_0) in the super cell can be obtained. These quasi-free electrons locate on the energy level of donors (E_D). The possibility of transition of quasi-free electrons from E_D to conduction band (E_C) follows the Boltzmann distribution. Thus, the concentration of free electrons (n) for conductance can be calculated by $n=n_0\exp[-(E_C-E_D)/kT]$, where k and T are the Boltzmann constant and operating temperature, respectively. As shown in Fig. 5(a), there is no specific position of E_D in defective

SnO_2 super cells because the whole band gap is filled by the donor energy levels. For convenience in discussion, the weighted average of the donor energy levels is considered as the eigenvalue of E_D. The position of E_D under E_C (E_C-E_D) is dependent on crystallite size, as Fig. 5(b). Then, the electron concentration at room temperature can be calculated, as illustrated in Fig. 6(b). So it is possible to calculated the resistivity (ρ) by using $\rho=1/nq\mu$, where q is the elementary charge and μ is the mobility of electrons (200 $cm^2/V\cdot S$ [57]). The resistivity is therefore illustrating a negative size effect in the volume-depleted crystallite, as shown in Fig. 6(b), though the number of quasi-free electron decreases with reducing crystallite size.

In the discussion above, the grain size effects on gas-sensitive SnO_2 quantum dots are investigated by both experimental and computational methods. As shown in Fig. 6(a), the size effects on sensor resistance and response to the reducing gas are illustrated for the grains larger than 2 nm. Considering the depletion layer width of approximate 4 nm, the size effects of grains with volume and partial depletion are revealed. However, it is very difficult to prepare SnO_2 QDs with crystallite size below 2 nm. Hence, to extend the discussion of size effects on volume-depleted grains, the DFT calculation is employed as a supplementary method to illustrate the size effect on the electron concentration and resistivity based on the defective super cells with various dimensions of 0.4-1.6 nm, as shown in Fig. 6(b). The resistivity of crystallites smaller than 2 nm demonstrates the same negative size effect as the resistance of the experimental grains. Thus, the full image of grain size effect is provided by combining the experimental and computational results. For the SnO_2 semiconductor, the resistance(resistivity) has a monotonically negative size effect while the sensor response reaches the maximum when the grain radius is equal to the depletion layer width. It is reserved that the DFT simulated results may deviate from the actuality

due to the presumptions in parameter settings in the calculation model, such as the stoichiometry and the number of adsorbed oxygen species.

It is noted that the crystallographic changes may occur during the reducing of grain size, accompanied by the changes in the concentration of defects and quasi-free electrons. A pronounced faceting would start to take place when the grain size is below 8-10 nm [43]. This transformation may potentially influence the surface properties of crystallites, which determine the adsorption-desorption processes of oxygen species. However, it is concluded that the (110) facet in the SnO_2 system has the lowest energy among other facets [58]. Therefore, the (110) facet is the most likely grain surface in the polycrystalline composite. Despite to the possible faceting, the gas-sensing mechanism of semiconductors is still valid in the SnO_2 QD gas sensors.

As proposed by N. Yamazoe, a classic gas-sensing mechanism of semiconductors consists of three parts, namely the receptor function, the transducer function and the utility factor [59]. In the mathematical expressions, the operating temperature is a fundamental factor that determines the sensor properties. The gas-sensing mechanism do not consider the operating temperature as a special factor and so it is valid whenever the gas sensor is under room temperature or a higher temperature. The receptor function describes how an individual grain responds to the stimulate gas. It includes several aspects, such as the grain size effect, the number and types of adsorbed oxygen, the density of donors, the width of depletion layer and so on. According to the temperature programmed desorption chromatograms, the adsorbed oxygen species of O_2, O_2^-, O^- and O^{2-} start to desorb around 80, 150, 560 and above 600 ^oC, respectively [60]. The similar result is concluded that the adsorbed oxygen would be removed over 250 ^oC [61]. Thus, it is possible for these oxygen species to adsorb on the grain surface at low temperature, even at room temperature.

However, only chemical adsorbed species are able to seize electrons in SnO_2 grains to complete the gas-sensing mechanism when they release the captured electrons back to grains after the exposure to the reducing gas. Thus, the physical adsorption of oxygen is not taken into consideration because of its minor impacts on sensor response. In the cutting-edge gas sensors operated at room temperature, three chemical adsorbed oxygen species make joint contribution to the sensor response. Hence, it is necessary to discuss the grain size effect of the advanced sensors with partial/volume-depleted nano-sized grains. Nevertheless, the contribution of each type of oxygen species is expected to be discussed in further investigations. Moreover, the humidity can make impacts on the type of adsorbates [37]. In case of low humidity (less than 0.01%), the O^{2-} type dominates over the O^- type. However, the formation of O^{2-} ions is suppressed and replaced by only O^- ions. Therefore, the operating temperature and humidity may influence the gas-sensing properties of semiconductors by changing the type and number of adsorbed oxygen. To minimize the impacts from aerial humidity, the dry air is used as the carrier gas during the sensor characterization.

Another two parameters in the utility factor are the pore size and film thickness, which dominate the gas diffusion process. The thickness of the present spin-coated thin film is 102 nm, which is identical throughout the discussion of size effect. The pore size, which is difficult to be observed by the SEM characterization, is considered to be the same order of magnitude as the grain size [23]. According to the mathematical functions of the utility factor [39,40], the sensor response is of positive dependence on the pore size because the increasing pore size benefits for the diffusion of the target gas inside the thin film. Thus, the size effect observed in this work involves the circumstance that the thin film has the approximately same size of grains and pores.

If the pore size is assumed to be identical in the thin films with various grain sizes, it is expected a more significant size effect on the response in the semiconductor gas sensors.

4. Conclusions

In conclusion, the present work discusses the grain size effect on electrical and gas-sensing properties of SnO_2 QDs by both experimental and computational methods. The resistance shows a monotonically negative size effect while the response reaches the optimization when the grain radius is comparable to the depletion layer width. It is of equal importance for the gas sensor design that the control of grain size and depletion layer width. The computational discussion concluded that both of E_C-E_D and quasi-free electron number decrease with size and their opposite contributions on conductance lead to a negative size effect of resistivity in volume-depleted SnO_2 crystallites. This work has contributed a comprehensive understanding of grain size effect of gas-sensitive semiconductor. The full image of size effects from partial depletion to volume depletion is described.

Acknowledgements

This research was funded by the National Natural Science Foundation of China (No. 11704055 and 31670516), the Liaoning Natural Science Foundation (No. 20180510021, the Joint Research Fund Liaoning-Shenyang National Laboratory for Materials Science), the Dalian High-level Talents Innovation Supporting Program (No. 2017RQ073), the Fundamental Research Funds for the Central Universities (No. 3132019348 and 3132020209) and the Large Instruments and Facilities Shared Foundation of Dalian Maritime University.

References

[1] T. Seiyama, A. Kato, K. Fujiishi, M. Nagatani, A new detector for gaseous components

using semiconductive thin films, Analytical Chemistry, 34 (1962) 1502-1503.

[2] Armin Jerger, Heinz Kohler, Frank Becker, Hubert B. Keller, Rolf Seifert, New applications of tin oxide gas sensors : II. Intelligent sensor system for reliable monitoring of ammonia leakages, Sensors and Actuators B: Chemical, 81 (2002) 301-307.

[3] R. Rella, P. Siciliano, S. Capone, M. Epifani, L. Vasanelli, A. Licciulli, Air quality monitoring by means of sol-gel integrated tin oxide thin films, Sensors and Actuators B: Chemical, 58 (1999) 283-288.

[4] Arturo Ortega, Santiago Marco, Alex Perera, Teodor Šundic, Antonio Pardo, Josep Samitier, An intelligent detector based on temperature modulation of a gas sensor with a digital signal processor, Sensors and Actuators B: Chemical, 78 (2001) 32-39.

[5] G. Korotcenkov, B.K. Cho, Bulk doping influence on the response of conductometric SnO_2 gas sensors: Understanding through cathodoluminescence study, Sensors and Actuators B: Chemical, 196 (2014) 80–98.

[6] N. Bârsan, M. Hübner, U. Weimar, Conduction mechanisms in SnO_2 based polycrystalline thick film gas sensors exposed to CO and H_2 in different oxygen backgrounds, Sensors and Actuators B: Chemical, 157 (2011) 510–517.

[7] Zhaoxia Zhai, Jianqiao Liu, Guohua Jin, Chuyao Luo, Qiuxuan Jiang, Yuqing Zhao, Characterization and gas sensing properties of copper-doped tin oxide thin films deposited by ultrasonic spray pyrolysis, Materials Science, 22 (2016) 201-204.

[8] Jae-Hun Kim, Ali Mirzaei, Hyoun Woo Kim, Sang Sub Kim, Improving the hydrogen sensing properties of SnO_2 nanowire-based conductometric sensors by Pd-decoration, Sensors and Actuators B: Chemical, 285 (2019) 358-367.

[9] Z. Song, Z. Huang, J. Liu, Z. Hu, J. Zhang, G. Zhang, F. Yi, S. Jiang, J. Lian, J. Yan, Fully stretchable and humidity-resistant quantum dot gas sensors, ACS Sensors, 3 (2018) 1048-1055.

[10] Huan Liu, Songman Xu, Min Li, Gang Shao, Huaibing Song, Wenkai Zhang, Wendian Wei, Mingze He, Liang Gao, Haisheng Song, Chemiresistive gas sensors employing solution-processed metal oxide quantum dot films, Applied Physics Letters, 105 (2014) 766.

[11] Huan Liu, Min Li, Oleksandr Voznyy, Long Hu, Qiuyun Fu, Dongxiang Zhou, Zhe Xia, Edward H Sargent, Jiang Tang, Physically flexible, rapid-response gas sensor based on colloidal quantum dot solids, Advanced Materials, 26 (2014) 2718-2724.

[12] Qi Yan, Liang Gao, Jiang Tang, Huan Liu, Flexible and stretchable photodetectors and gas sensors for wearable healthcare based on solution-processable metal chalcogenides, Journal of Semiconductors, 40 (2019) 111604.

[13] Jingyao Liu, Zhixiang Hu, Yuzhu Zhang, Hua-Yao Li, Naibo Gao, Zhilai Tian, Licheng Zhou, Baohui Zhang, Jiang Tang, Jianbing Zhang, Fei Yi, Huan Liu, MoS_2 nanosheets sensitized with quantum dots for room-temperature gas sensors, Nano-micro Letters, 12 (2020) 59.

[14] Min Li, Jingting Luo, Chen Fu, Hao Kan, Zhen Huang, Wangman Huang, Shuqin Yang, Jianbing Zhang, Jiang Tang, Yongqing Fu, Honglang Li, Huan Liu, PbSe quantum dots-based chemiresistors for room-temperature NO_2 detection, Sensors and Actuators B: Chemical, 256 (2018) 1045-1056.

[15] L.A. Patil, D.R. Patil, Heterocontact type CuO-modified SnO_2 sensor for the detection of a ppm level H_2S gas at room temperature, Sensors and Actuators B: Chemical, 120 (2006)

316-323.

[16] Shuping Gong, Jing Xia, Jianqiao Liu, Dongxiang Zhou, Highly sensitive SnO_2 thin film with low operating temperature prepared by sol-gel technique, Sensors and Actuators B: Chemical, 134 (2008) 57-61.

[17] C. Xu, J. Tamaki, N. Miura, N. Yamazoe, Grain size effects on gas sensitivity of porous SnO_2-based elements, Sensors and Actuators B: Chemical, 3 (1991) 147-155.

[18] G Korotcenkov, S-D Han, BK Cho, V Brinzari, Grain size effects in sensor response of nanostructured SnO_2-and In_2O_3-based conductometric thin film gas sensor, Critical Reviews in Solid State and Materials Sciences, 34 (2009) 1-17.

[19] SG Ansari, P Boroojerdian, SR Sainkar, RN Karekar, RC Aiyer, SK Kulkarni, Grain size effects on H_2 gas sensitivity of thick film resistor using SnO_2 nanoparticles, Thin Solid Films, 295 (1997) 271-276.

[20] ZA Ansari, SG Ansari, T Ko, J-H Oh, Effect of MoO_3 doping and grain size on SnO_2-enhancement of sensitivity and selectivity for CO and H_2 gas sensing, Sensors and Actuators B: Chemical, 87 (2002) 105-114.

[21] Gong Zhang, Meilin Liu, Effect of particle size and dopant on properties of SnO_2-based gas sensors, Sensors and Actuators B: Chemical, 69 (2000) 144-152.

[22] Avner Rothschild, Yigal Komem, The effect of grain size on the sensitivity of nanocrystalline metal-oxide gas sensors, Journal of Applied Physics, 95 (2004) 6374-6380.

[23] Tetsuya Kida, Shuhei Fujiyama, Koichi Suematsu, Masayoshi Yuasa, Kengo Shimanoe, Pore and particle size control of gas sensing films using SnO_2 nanoparticles synthesized by seed-mediated growth: design of highly sensitive gas sensors, The Journal of Physical

Chemistry C, 117 (2013) 17574-17582.

[24] Koichi Suematsu, Masayoshi Yuasa, Tetsuya Kida, Noboru Yamazoe, Kengo Shimanoe, Effects of crystallite size and donor density on the sensor response of SnO_2 nano-particles in the state of volume depletion, Journal of the Electrochemical Society, 159 (2012) J136.

[25] Jianqiao Liu, Guohua Jin, Zhaoxia Zhai, Faheema Fairuj Monica, Xuesong Liu, Numeral description of grain size effects of tin oxide gas-sensitive elements and evaluation of depletion layer width, Electronic Materials Letters, 11 (2015) 457-465.

[26] Noboru Yamazoe, Kengo Shimanoe, Roles of shape and size of component crystals in semiconductor gas sensors II. Response to NO_2 and H_2, Journal of the Electrochemical Society, 155 (2008) J93-J98.

[27] Noboru Yamazoe, Kengo Shimanoe, Roles of shape and size of component crystals in semiconductor gas sensors I. Response to oxygen, Journal of the Electrochemical Society, 155 (2008) J85-J92.

[28] Jianqiao Liu, Yiting Lu, Xiao Cui, Guohua Jin, Zhaoxia Zhai, Effect of depletion layer width on electrical properties of semiconductive thin film gas sensor: a numerical study based on the gradient-distributed oxygen vacancy model, Applied Physics A, 122 (2016) 146.

[29] N. Yamazoe, K. Shimanoe, Theory of power laws for semiconductor gas sensors, Sensors and Actuators B: Chemical, 128 (2008) 566-573.

[30] Yamazoe Noboru, Shimanoe Kengo, Receptor function and response of semiconductor gas sensor, Journal of Sensors, 2009 (2009) 21.

[31] Jianqiao Liu, Shuping Gong, Qiuyun Fu, Yi Wang, Lin Quan, Zhaojie Deng, Binbin Chen, Dongxiang Zhou, Time-dependent oxygen vacancy distribution and gas sensing

characteristics of tin oxide gas sensitive thin films, Sensors and Actuators B: Chemical, 150 (2010) 330-338.

[32] Jianqiao Liu, Shuping Gong, Lin Quan, Zhaojie Deng, Huan Liu, Dongxiang Zhou, Influences of cooling rate on gas sensitive tin oxide thin films and a model of gradient distributed oxygen vacancies in SnO_2 crystallites, Sensors and Actuators B: Chemical, 145 (2010) 657-666.

[33] Jianqiao Liu, Xuesong Liu, Zhaoxia Zhai, Guohua Jin, Qiuxuan Jiang, Yuqing Zhao, Chuyao Luo, Lin Quan, Evaluation of depletion layer width and gas-sensing properties of antimony-doped tin oxide thin film sensors, Sensors and Actuators B: Chemical, 220 (2015) 1354-1360.

[34] Jianqiao Liu, Zhaoxia Zhai, Guohua Jin, Yuan Li, Faheema Fairuj Monica, Xuesong Liu, Simulation of the grain size effect in gas-sensitive SnO_2 thin films using the oxygen vacancy gradient distribution model, Electronic Materials Letters, 11 (2015) 34-40.

[35] C. Malagù, V. Guidi, M. Stefancich, M.C. Carotta, G. Martinelli, Model for Schottky barrier and surface states in nanostructured n-type semiconductors, Journal of Applied Physics, 91 (2002) 808-814.

[36] Noboru Yamazoe, Koichi Suematsu, Kengo Shimanoe, Extension of receptor function theory to include two types of adsorbed oxygen for oxide semiconductor gas sensors, Sensors and Actuators B: Chemical, 163 (2012) 128-135.

[37] Noboru Yamazoe, Koichi Suematsu, Kengo Shimanoe, Two types of moisture effects on the receptor function of neat tin oxide gas sensor to oxygen, Sensors and Actuators B: Chemical, 176 (2013) 443-452.

[38] Noboru Yamazoe, Kengo Shimanoe, Basic approach to the transducer function of oxide semiconductor gas sensors, Sensors and Actuators B: Chemical, 160 (2011) 1352-1362.

[39] Jianqiao Liu, Shuping Gong, Jing Xia, Lin Quan, Huan Liu, Dongxiang Zhou, The sensor response of tin oxide thin films to different gas concentration and the modification of the gas diffusion theory, Sensors and Actuators B: Chemical, 138 (2009) 289-295.

[40] G. Sakai, N. Matsunaga, K. Shimanoe, N. Yamazoe, Theory of gas-diffusion controlled sensitivity for thin film semiconductor gas sensor, Sensors and Actuators B: Chemical, 80 (2001) 125-131.

[41] Jianqiao Liu, Qianru Zhang, Weiting Xue, Haipeng Zhang, Yu Bai, Liting Wu, Zhaoxia Zhai, Guohua Jin, Fluorescence characteristics of aqueous synthesized tin oxide quantum dots for the detection of heavy metal ions in contaminated water, Nanomaterials, 9 (2019) 1294.

[42] Jianqiao Liu, Weiting Xue, Guohua Jin, Zhaoxia Zhai, Jiarong Lv, Wusong Hong, Yuzhen Chen, Preparation of tin oxide quantum dots in aqueous solution and applications in semiconductor gas sensors, Nanomaterials, 9 (2019) 240.

[43] Jianqiao Liu, Yichen Nie, Weiting Xue, Liting Wu, Hao Jin, Guohua Jin, Zhaoxia Zhai, Ce Fu, Size effects on structural and optical properties of tin oxide quantum dots with enhanced quantum confinement, Journal of Materials Research and Technology, 9 (2020) 8020-8028.

[44] V. Milman, B. Winkler, J. A. White, C. J. Pickard, M. C. Payne, E. V. Akhmatskaya, R. H. Nobes, Electronic structure, properties, and phase stability of inorganic crystals: A pseudopotential plane-wave study, International Journal of Quantum Chemistry, 77 (2015) 895-910.

[45] Jianqiao Liu, Qianru Zhang, Xinyue Tian, Ye Hong, Yichen Nie, Ningning Su, Guohua Jin, Zhaoxia Zhai, Ce Fu, Highly efficient photocatalytic degradation of oil pollutants by oxygen deficient SnO_2 quantum dots for water remediation, Chemical Engineering Journal, 404 (2021) 127146.

[46] P. A. Mulheran, J. H. Harding, The stability of SnO_2 surfaces, Modelling and Simulation in Materials Science and Engineering, 1 (1992) 39-43.

[47] J. Oviedo, M. J. Gillan, . Energetics and structure of stoichiometric SnO_2 surfaces studied by first-principles calculations, Surface Science, 463 (2000) 93-101.

[48] Yanping Chen, Hongwei Qin, Jifan Hu, CO sensing properties and mechanism of Pd doped SnO_2 thick-films, Applied Surface Science, 428 (2018) 207-217.

[49] S.R. Morrison, Mechanism of semiconductor gas sensor operation, Sensors and Actuators, 11 (1987) 283-287.

[50] Jianqiao Liu, Fengjiao Gao, Liting Wu, Haipeng Zhang, Wusong Hong, Guohua Jin, Zhaoxia Zhai, Ce Fu, Size effect on oxygen vacancy formation and gaseous adsorption in ZnO nanocrystallites for gas sensors: a first principle calculation study, Applied Physics A, 126 (2020) 454.

[51] Hitoshi Seki, Nobuo Ishisawa, Nobuyasu Mizutani, Masanori Kato, High temperature structures of the rutile-type oxides, TiO_2 and SnO_2, Journal of the Ceramic Association Japan, 92 (1984) 219-223.

[52] N. Yamazoe, Y. Kurokawa, T. Seiyama, Effects of additives on semiconductor gas sensors, Sensors and Actuators, 4 (1983) 283-289.

[53] Jianqiao Liu, Yiting Lu, Xiao Cui, Yuncong Geng, Guohua Jin, Zhaoxia Zhai,

Gas-sensing properties and sensitivity promoting mechanism of Cu-added SnO_2 thin films deposited by ultrasonic spray pyrolysis, Sensors and Actuators B: Chemical, 248 (2017) 862-867.

[54] H. Liu, S. Wu, S. Gong, J. Zhao, J. Liu, D. Zhou, Nanocrystalline In_2O_3-SnO_2 thick films for low-temperature hydrogen sulfide detection, Ceramics International, 37 (2011) 1889-1894.

[55] Nguyen Van Toan, Nguyen Viet Chien, Nguyen Van Duy, Hoang Si Hong, Hugo Nguyen, Nguyen Duc Hoa, Nguyen Van Hieu, Fabrication of highly sensitive and selective H_2 gas sensor based on SnO_2 thin film sensitized with microsized Pd islands, Journal of Hazardous materials, 301 (2016) 433-442.

[56] Jianqiao Liu, Yinglin Gao, Xu Wu, Guohua Jin, Zhaoxia Zhai, Huan Liu, Inhomogeneous oxygen vacancy distribution in semiconductor gas sensors: Formation, migration and determination on gas sensing characteristics, Sensors, 17 (2017) 1852.

[57] Z. M. Jarzebski, J. P. Marton, Physical properties of SnO_2 materials, Journal of the Electrochemical Society, 123 (1976) 199C-205C.

[58] J. Oviedo, M. J. Gillan, Energetics and structure of stoichiometric SnO_2 surfaces studied by first-principles calculations, Surface Science, 463 (2000) 93-101.

[59] N. Yamazoe, K. Shimanoe, New perspectives of gas sensor technology, Sensors and Actuators B: Chemical, 138 (2009) 100-107.

[60] N. Yamazoe, J. Fuchigami, M. Kishikawa, T. Seiyama, Interactions of tin oxide surface with O_2, H_2O and H_2, Surface Science, 86 (1979) 335-344.

[61] S.R. Morrison, Semiconductor gas sensors, Sensors and Actuators, 2 (1982) 329-341.

Figure captions

Fig. 1 Schematic drawing of (a) the SnO_2 QD thin film gas sensor with Ag interdigital electrodes on the alumina substrate and (b) the computer-controlled characterization system for gas sensors.

Fig. 2 Crystal structure and morphology of size-controllable SnO_2 QDs with hydrothermal treatment time of 0-20 h: (a) XRD patterns of SnO_2 QDs as well as the standard diffraction pattern of SnO_2; (b) Estimated crystallite size and grain size; (c) EDS spectrum; (d) HRTEM, (e) SEM and (f) cross section observations.

Fig. 3 Gas-sensing characteristics of SnO_2 QDs: (**a**) Dependences of resistance and response on hydrothermal treatment time; (**b**) Transient response to continuous and repeated injections of H_2 and correlation of response against gas concentration in the linear and logarithmic coordinates.

Fig. 4 Structural models for first principle calculation of (a) 1×1×2 and (b) 3×3×5 SnO_2 super cells with 25% oxygen vacancies and adsorbed oxygen on the surface.

Fig. 5 (a) Density of states of SnO_2 super cells and (b) the dependence of E_C-E_D and adsorption energy of oxygen species on crystallite size.

Fig. 6 Grain size effect on the electrical and gas-sensing properties of SnO_2 QDs: (**a**) Experimental resistance and response of SnO_2 grains with volume and partial depletion; (**b**) Computational resistivity and electron concentration in SnO_2 crystallites.

Table captions

Tab. 1. Mulliken population distribution of O and Sn atoms in the computational model with various dimensions.

Table 1. Mulliken population distribution of O and Sn atoms in the computational model with various dimensions.

Structure	Size (nm)	O charge (e)	Sn charge (e)	Quasi-free electron (e)
1×1×2	0.474	-0.71	1.65	0.585
2×2×2	0.637	-0.80	1.59	0.390
2×2×3	0.956	-0.81	1.58	0.365
3×3×3	1.421	-0.84	1.55	0.290
3×3×5	1.593	-0.86	1.51	0.220

(a)

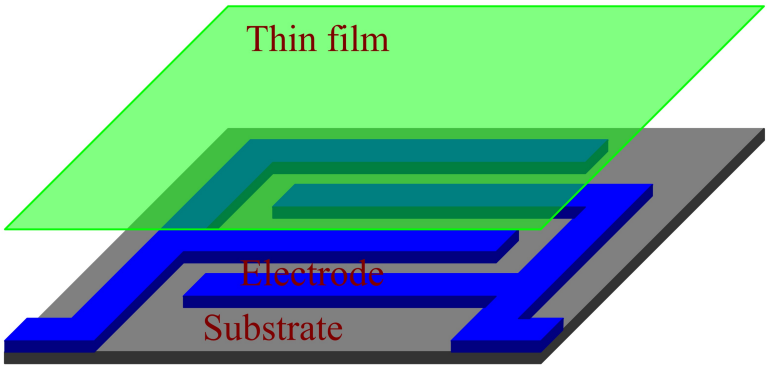

(b)

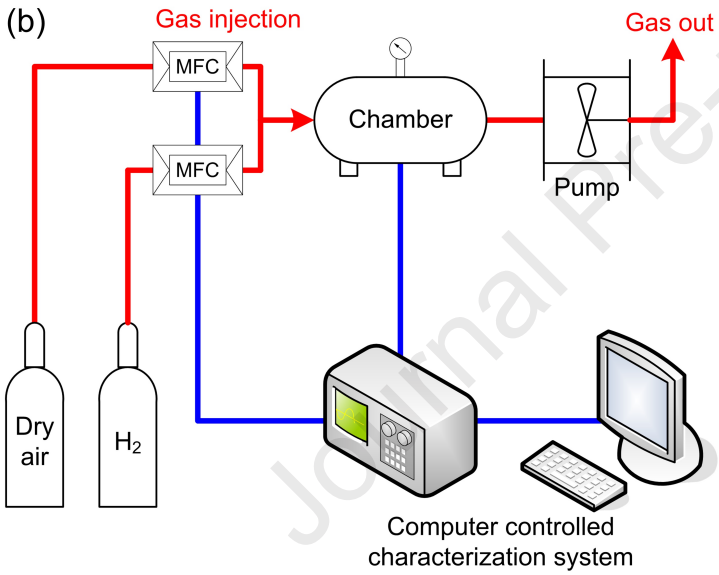

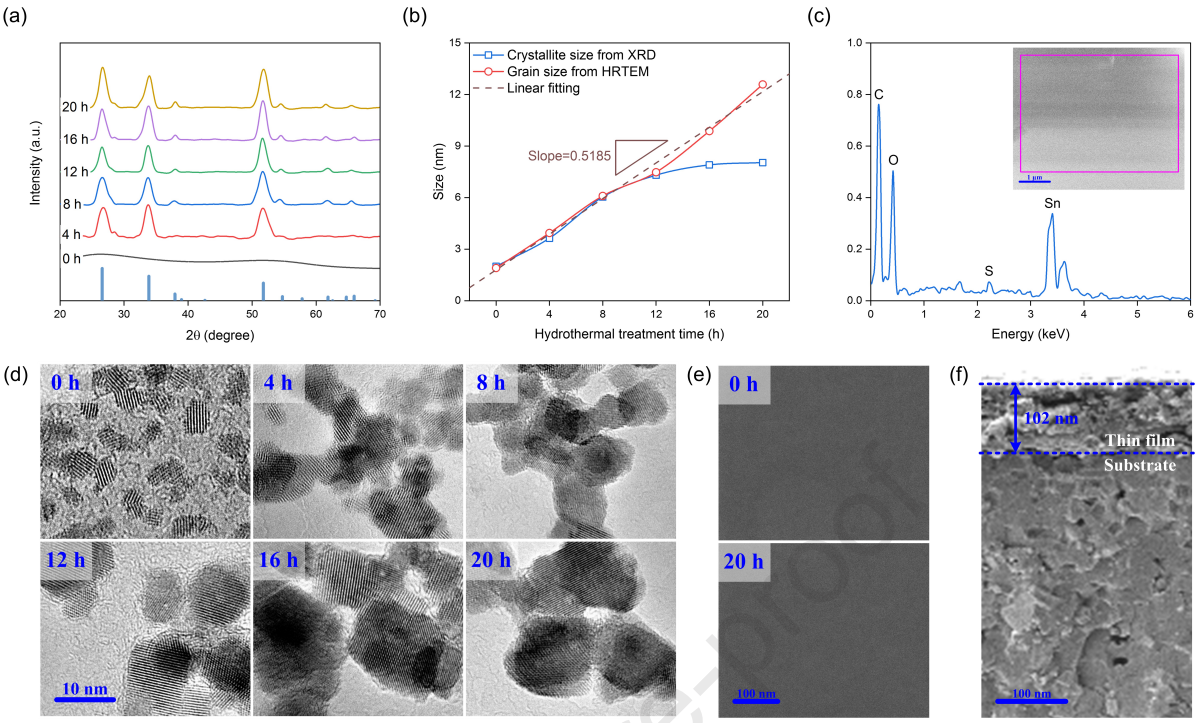

(a)

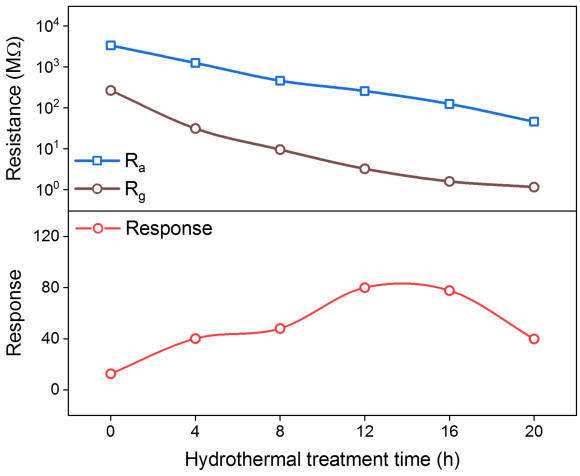

(b)

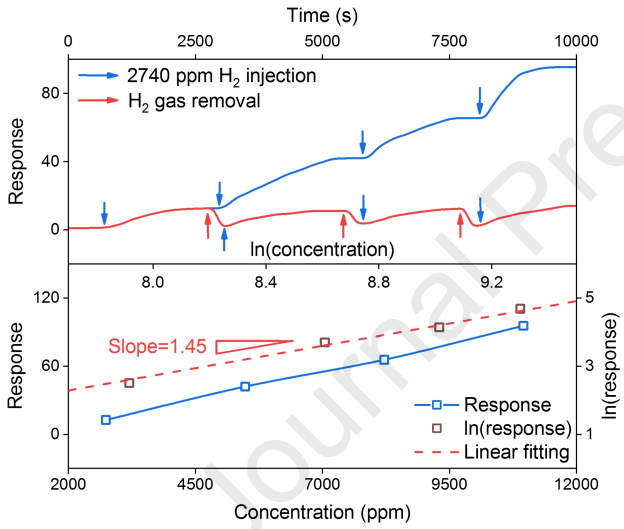

(a)

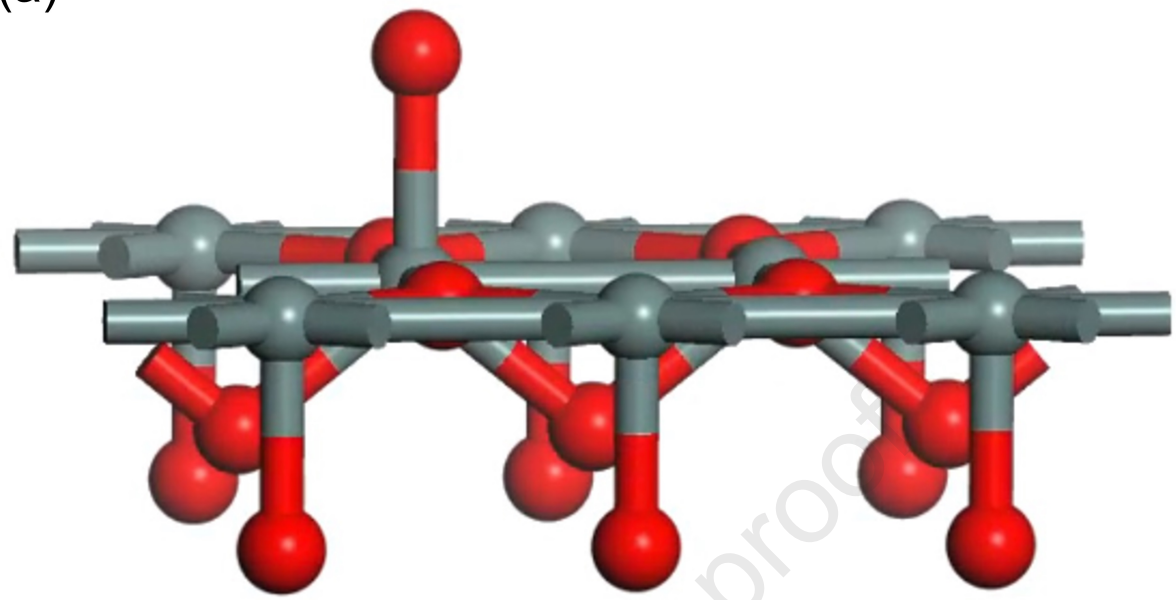

(b)

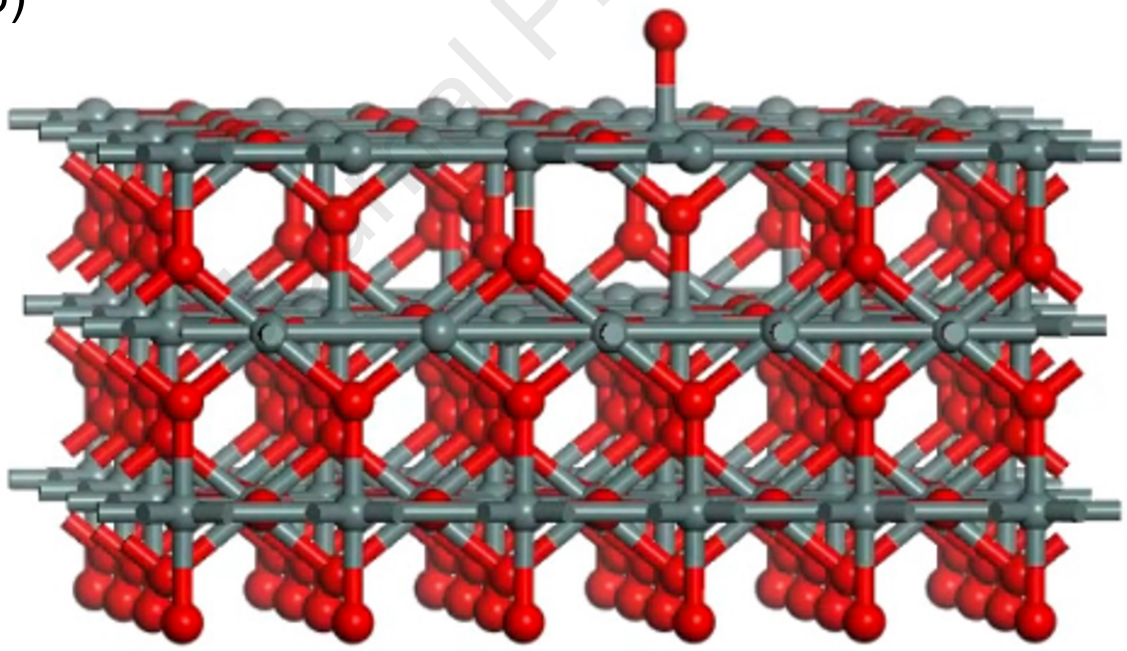

(a)

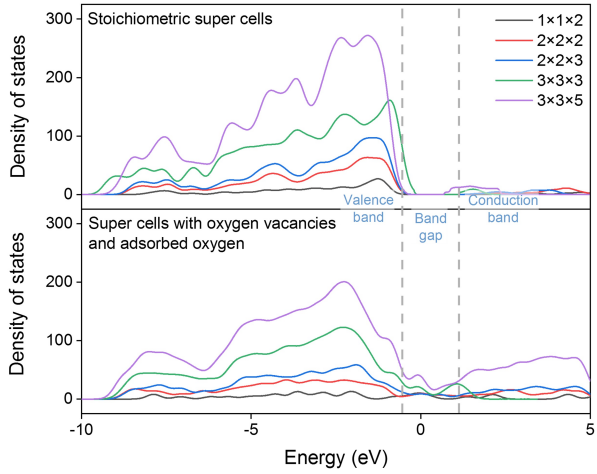

(b)

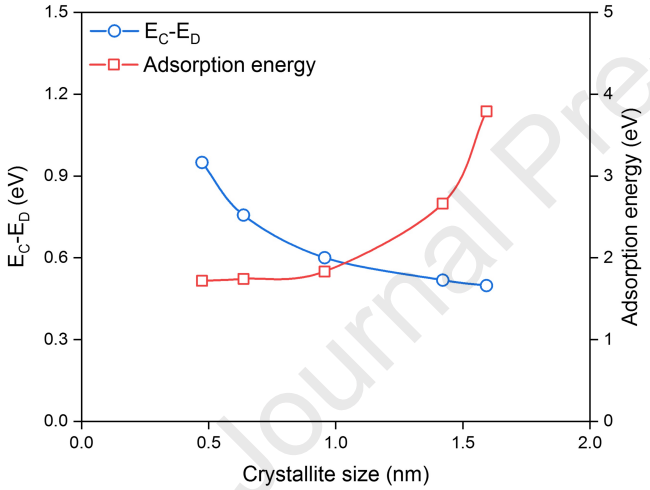

(a)

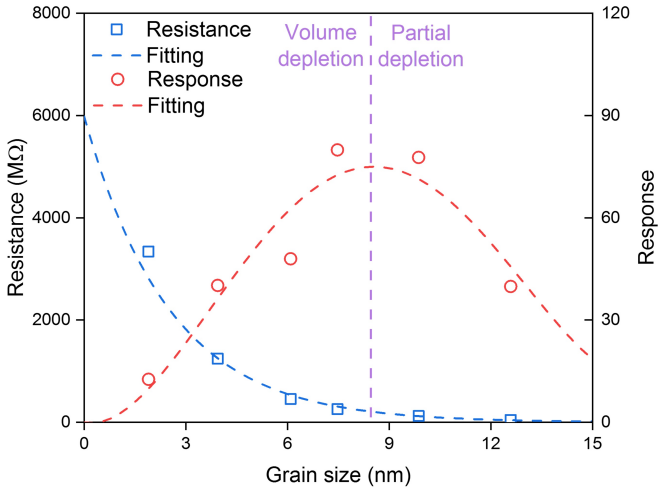

(b)

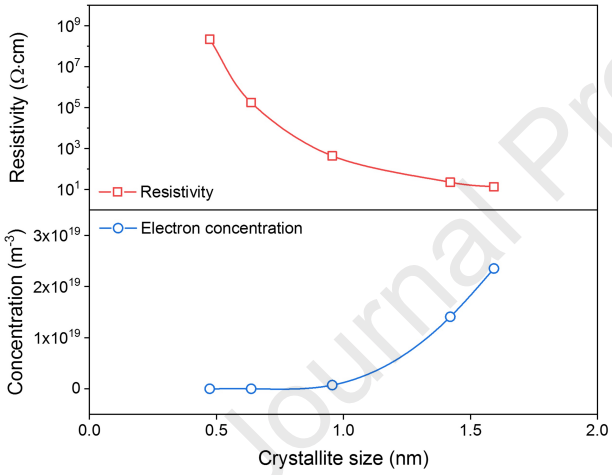

Declaration of interests

√ The authors declare that they have no known competing financial interests or personal relationships that could have appeared to influence the work reported in this paper.

☐The authors declare the following financial interests/personal relationships which may be considered as potential competing interests: